Published in final edited form as:
Biotechnol Bioeng. 2012 June ; 109(6): 1571–1582. doi:10.1002/bit.24412.

Biomimetic Micropatterned Multi-channel Nerve Guides by Templated Electrospinning

Eric Jeffries and **Yadong Wang***
414 Benedum Hall, 3700 O'Hara Street, Pittsburgh, PA 15261

Abstract

This report describes a new approach for fabricating micro-channels within three-dimensional electrospun constructs. These key features serve to mimic the fascicular architecture and fibrous extracellular matrix found in native nerve. Both electrospun fibers and multi-channeled structure nerve guides have become areas of increasing interest for their beneficial roles in nerve repair. However, to the best of our knowledge, this is the first report of a guide that incorporates both. Multiple parallel channels provide a greater number of defined paths and increased surface area compared to cylindrical guides. Additionally, the fibrous nature of electrospun fibers permits better mass transport than solid-walled constructs. The flexible fabrication scheme allows tailoring of nerve guide parameters such as channel diameters ranging from 33-176μm and various wall thicknesses. Channel and fiber structures were assessed by optical and electron microscope images. Geometric calculations estimated a porosity of over 85% for these guides with 16% or less from the channels. In vitro culture with Schwann cells demonstrated cellular infiltration into channels with restricted migration between fibers. Finally, cell proliferation and survival throughout the guide indicates that this design warrants future in vivo examination.

Keywords

Nerve guide; topographical guidance; nerve regeneration; polycaprolactone; electrospinning; Schwann cell

Introduction

Peripheral nerve injuries accompany approximately 2.8% of trauma patients, or 100,000 people in the US and Europe annually (Chiona et al. 2009; Noble et al. 1998). These injuries cause loss of sensation and muscle function, in addition to painful neuropathies (Yan et al. 2009). Due to an innate regenerative capacity of peripheral nerves, injuries yielding insignificant or no loss of axon continuity typically repair naturally (Campbell 2008; Schlosshauer et al. 2006). However, severe injuries causing complete nerve transection require surgical intervention. Small gaps are surgically anastamosed without tension while larger gaps are bridged by an implant to provide structural, mechanical, and biochemical support (Kehoe et al. 2011). Although autografts produce donor site morbidity and yield incomplete or inconsistent recovery, they are still preferred over alternative nerve guides and remain the clinical gold standard (Gu et al. 2010). Consequently, prosthetic alternatives capable of matching or exceeding the performance of autografts are a highly active area of research (Gu et al. 2010; Schmidt and Leach 2003).

*Correspondence to phone: 412-624-7196, yaw20@pitt.edu.

Clinically-available nerve grafts are limited to single-lumen conduits constructed of collagen, poly(glycolic acid), poly (D,L-lactide-co-ε-caprolactone), poly(vinyl alcohol), or decellularized extracellular matrix (ECM) and yield outcomes inferior to autografts (Kehoe et al. 2011). Moderate experimental success has been achieved by nerve autografts and muscle basal lamina(Flynn et al. 2003). We believe this may be due in part to the confinement of the nerve within the complex multi-channel structure of the basal lamina. Through numerous fabrication methods researchers have attempted to mimic these designs but fail to achieve the same success (Yao et al. 2010).

To address this challenge, we designed the first multi-channel nerve guide composed entirely of electrospun fibers intended to mimic the fascicular architecture and extracellular matrix respectively. Our design satisfies 3 design criteria that have not been achieved by previous methods. 1) Our design incorporates a high density of channels which is uncommon in other templating approaches. 2) We have greater control of channel size and regularity compared to freeze drying methods. 3) Our design consists of interconnected spaces between fibers instead of the solid walls created by casting methods. Additionally, we can customize many aspects of the design such as fiber diameter, composition, and alignment, in addition to channel diameter and spacing. We anticipate this design being especially useful for nerve repair in the future by incorporating aligned fibers, which can guide axon growth.

Materials and Methods

Electrospinning

A 14% polycaprolactone (PCL) (Mn=80,000, Sigma) solution was prepared by dissolving PCL pellets in 5:1 trifluoroethanol:water at room temperature under agitation overnight(Cao et al. 2009). Random fibers were deposited on the aluminum face of a custom collector (Fig 2A) during horizontal stationary electrospinning (Fig 1A). The collector also had two fine tooth combs (18 teeth per cm) attached to the sides to align sutures in a regularly-spaced parallel pattern. Radially-aligned fibers were deposited around the guide via rotating electrospinning (Fig 1B) to prevent unraveling. For both electrospinning methods, the collector was placed 25 cm from the needle and the polymer solution was pumped through a 21 gauge needle at a flow rate of $25\mu l \cdot min^{-1}$. Electrostatic potentials of 15 kV positive and 10 kV negative were attached to the needle and collector respectively.

Nerve Guide Preparation

A random mesh of PCL fibers were deposited on the aluminum face of a collector by stationary electrospinning a set volume, V_1 μL, of PCL solution (Fig 2A). Sutures were woven taut around the teeth on the collector to form N parallel strand templates atop the electrospun fibers (Fig 2B). Sutures were covered with a second layer of random PCL fibers by electrospinning a set volume, V_2 μL (Fig 2C). The entire construct was placed in a vacuum chamber overnight to remove residual solvent. The thickness of each layer is adjusted by varying volumes V_1 and V_2 and the number of channels equals N.

After drying, the sutures were cut at both ends to release the electrospun mat from the collector (Fig 2D). The multilayered electrospun mat was rolled up parallel to the sutures and secured with two collagen sutures (Fig 2E). Recent designs used parafilm to secure the template strands rather than tying with sutures. The outside was then sealed with a thin sheath of aligned PCL microfibers by electrospinning 50μL PCL while rotating the nerve guide at 60 rpm in front of the collector (Fig 1B). This outer sheath helps to prevent nerve guide from unraveling. The patterning sutures were removed, creating aligned channels in their void. The nerve guide preparation was completed by trimming the guide to the desired

length by cutting each end (Fig 2F). This removes the peripheral regions of the electrospun mat with low fiber density. Prior to trimming the guide, it was soaked in deionized water (diH_2O) for 1 hour and frozen on dry ice. The integrity of the micro-channels was better maintained during sectioning if water was allowed to penetrate the nerve guide and frozen to mechanically support it during cutting. The nerve guides were stored in microcentrifuge tubes until use.

Porosity

The porosity of the guide, including channels, was estimated used the geometric equations outlined in the paper by Yang.(Yang et al. 2005b) Briefly, the porosity, P, is calculated from equation 1.

$$P=\left(1-\frac{V_p}{V_t}\right)*100 \quad (1)$$

V_p is the volume of the polymer and V_t is the total volume of the guide, obtained from the following equations.

$$V_p=\frac{m_t}{d_p} \quad (m_t\text{mass of total guide}) \quad (d_p\text{density of polymer}) \quad (2)$$

$$V_t=\pi r_t^2 * l \quad (r_t\text{radius of total guide}) \quad (l=\text{length}) \quad (3)$$

The term V_p/V_t in equation 1 represents the volume occupied by the polymer. Thus, one minus this value provides the volume of the free space in the guide including gaps between fibers and the channels. The volume (V_c) and percent porosity (P_c) contributed from the channels is also obtained from equations 4 and 5.

$$V_c=\pi r_c^2 * l * n \quad (r_c\text{radius of channel}) \quad (n=\text{number of channels}) \quad (4)$$

$$P_c=\left(\frac{V_c}{V_t-V_p}\right)*100 \quad (5)$$

Scanning electron microscope (SEM)

SEM samples were prepared by cutting thin (approximately 1-2 mm) transverse slices of nerve guides with a scalpel and adhering to an aluminum stub using carbon tape. The samples were dehydrated in a desiccator overnight. The samples were coated with 3nm of gold with a Cressington Sputter Coater and grounded to the stub with aluminum paint. Samples were imaged with a Jeol JSM-6330F SEM.

Analysis of electrospinning parameters

Reproducibility and layer thickness—Three guides were produced using V_1/V_2= 75 μL and 35 templates of 100 μm diameter. It should be noted that this was spun on a collector 7cm long and 4cm wide, so not all of the deposited fibers were in the portion used for the guide. The qualitative structure of 1-2 mm hydrated sections were observed on an Olympus SZX10 stereo microscope and compared to others where the layer thicknesses were varied such that V_1/V_2=40, V_1=40/V_2=100, and V_1/V_2=100. Additionally, porosities determined from the above equations were reported.

Channel diameter—A guide was fabricated using template diameters of 20, 70, 100 and 150μm. The number of templates and layer thicknesses were adjusted based on template size. Optical images of 1-2mm hydrated samples were again viewed an Olympus SZX10 stereo microscope. ImageJ was used to determine channel size via two orthogonal diameter measurements for 10 channels per transverse-section. Average channel diameter (+/-) standard deviation is reported.

Cell Culture

Rat Schwannoma cell line RT4-D6P2T (ATCC CRL-2768) was kindly provided by the Badylak lab. Cells were cultured with Dulbecco's Modified Eagle Medium (DMEM) (ATCC 30-2002) with 10% fetal bovine serum (FBS), 1% antibiotic/antimycotic (Cellgro 30-004-Cl) in incubators at 37°C and 5% carbon dioxide.

Nerve guides were sliced to lengths of 1.2 cm, sterilized by ethylene oxide, and washed in sterile 1X PBS for 2 days on an orbital shaker, changing PBS after the first day. Nerve guides were then incubated with 10μg/mL laminin solution at 37°C for 13 hours. Nerve guides were washed once in 1X phosphate buffer solution (PBS) prior to cell seeding.

Cells (passage #8) were trypsinized and resuspended at a concentrated 7,633 cells/μL. A 65μL solution of cell suspension was pipetted into each side of the guide for a total of 1×10^6 cells per guide. This not absorbed by the guide was pipette into each end a second time. Nerve guides were placed in 12 well plates and 1mL media was added to each well. The plates were placed in a 37°C incubator for 1 hour. Nerve guides were then placed on a shaker in the incubator for 1 hour before transferring to new 12-well plates to eliminate the large number of cells adhered to culture plate. Guides were incubated while shaking until evaluation at 4 and 11 day time points for 4',6-diamidino-2-phenylindole (DAPI) (n=3) and 3-(4,5-dimethylthiazol-2-yl)-2,5-diphenyltetrazolium bromide (MTT) (n=3).

Schwann cell SEM preparation—Guides containing cells were placed in a fixation solution (2.5% glutaraldehyde in 1X PBS) overnight at 4°C. Nerve guides were then dehydrated through serial dilution in 25, 30, 50, 70, 80, 90, 100 percent ethanol in water. This was followed by dehydration in 3:1, 1:1, and 1:3 (3 times) ethanol:hexamethyldisilazane (HDMS). Nerve guides were immersed for 15 minutes in each solution. The nerve guide was then left in 100 percent HDMS in fume hood overnight for complete drying. The nerve guide was cut at a 45 degree angle cross-section to reveal the interior of the guide. Samples were prepared on SEM stubs as previously described.

Live/Dead/DAPI—Live/dead solution was prepared by adding calcein AM (20μM) and ethidium homodimer (1μM) to DMEM without phenol red or FBS. Three nerve guides from each time point were washed three times with 1X PBS before incubating in1.5 mL live/dead solution for 3 hours. Guides were then cut in half, frozen in OCT, and sectioned on a microtome to produce transverse and longitudinal slices (8 μm thick). The cell nuclei were stained with DAPI mounting solution and viewed on a Nikon Eclipse Ti inverted microscope. Analysis focused on identifying cell infiltration (location of cells relative to channels) and proliferation (number of cells). Due to background staining associated with the guide fibers, no immunofluorescence was used. Image look-up table (LUT) minimum threshold and G-value were adjusted to improve the contrast so DAPI could be seen in relation to the structures in the guide.

MTT—Three nerve guides, three guides without cells, and calibration curve cells seeded at 1, 0.5, 0.25, and 0.125 million cells per tissue culture polystyrene (TCPS) well and acclimated for 3 hours in culture were used for the MTT assay. Each sample was washed

three times with 1X PBS to remove residual media containing phenol red. MTT solution (0.5mg/mL media without FBS or phenol red) was added to each well for 3 hours at 37°C. Small sections from the ends and center of the guides were section for imaging. Images did not clearly show MTT crystals and are not shown. DMSO was added to the remaining pieces of the seeded nerve guides and to the other samples. Mechanical disruption was applied to the seeded guides to solublize MTT trapped in the fibers. After 30 minutes, the solutions were removed and added to 96 well plates in triplicate for absorbance reading at 540nm.

Results and Discussion

Multi-channel electrospun design mimics nerve microstructure

Rationale for multi-channel design—An array of parallel microchannels is present in healthy nerves and preservation of this endoneurial structure is an optimistic indicator in the prognosis of nerve injuries (Campbell 2008). Therefore, the major goal of our design was to incorporate endoneurial-like structures in a nerve guide. Single lumen nerve guides aid regeneration by concentrating chemical signals and restricting infiltration of inflammatory cells (Kehoe et al. 2011). However, single lumen conduits fail to present a multi-channel structure like that of a native nerve. Furthermore, collapse of a single lumen conduit drastically impairs nerve repair (Yao et al. 2010).

Existing multi-channel designs—Multi-channeled nerve guides have been fabricated by a variety of methods including freeze drying, injection molding, thermally-induced phase separation (TIPS), electrodeposition, and various combinations of these methods (Ao et al. 2006; Bozkurt et al. 2007; de Ruiter et al. 2008; Flynn et al. 2003; George et al. 2009; He et al. 2009; Hu et al. 2009; Madaghiele et al. 2008; Stokols and Tuszynski 2004; Sundback et al. 2003; Wang et al. 2006; Yao et al. 2010). There are several key differences distinguishing our design from existing methods of producing multi-lumen guides. Our guide has electrospun fibers with an open porous structures to facilitate mass transport. Contrarily, mold casting, lithographic, and deposition techniques generate nerve guides with thick or continuous walls which are likely to limit mass transfer (Flynn et al. 2003; George et al. 2009; Stokols et al. 2006; Sundback et al. 2003; Wang and Huang 2008; Yao et al. 2010). Additionally, we report a high channel density, while many of these mold casting methods produce very few channels. Our fabrication scheme can create well-defined channels with a diameter as small as 33 μm. This can be contrasted with the other common methods such as freeze-drying, TIPS, and gas foaming which are porous but often lack control of channel size, orientation, and interconnectivity (Bozkurt et al. 2007; Hu et al. 2009; Madaghiele et al. 2008; Stokols and Tuszynski 2004). Other approaches capable of producing porous guides with defined channels are limited to 150 μm minimum diameter rods used to make the channels and the difficulties associated with aligning and removing rod templates with large aspect ratios (He et al. 2009; Wang et al. 2006; Yang et al. 2005b). Finally, our layered fabrication scheme will allow us to make future modifications to incorporate aligned fibers within channels to provide nanometer-scale topographical guidance. Aligned electrospun fibers have demonstrated utility in directing nerve outgrowth as well as inducing morphology changes (Chew et al. 2007; Kim et al. 2008; Madduri et al. 2010; Wang et al. 2010; Yang et al. 2005a; Yao et al. 2009). The ability to perform this type of modification has not been demonstrated by other methods, making our approach unique (Hadlock et al. 2000).

Rationale for electrospinning—Native nerve is surrounded by an extracellular matrix that is fibrous and porous (Zhang et al. 2010). The process of electrospinning has gained much attention in tissue engineering in recent years for its ability to controllably produce

sub-micron to micron-sized fibers that mimic the fibrous nature of ECM (Agarwal et al. 2008). However, since electrospinning is best-suited for production of two-dimensional meshes, incorporation into three-dimensional constructs appropriate for nerve regeneration has been difficult and limited (Jha et al. 2011).

Current electrospinning methods—Existing methods of incorporating electrospun fibers into nerve guides radially- or axially-align fibers on the circumference of a hollow conduit or insert flat sheets into the lumen (Biazar et al. 2010; Chew et al. 2007; Clements et al. 2009). These methods do not utilize the entire cross-sectional area for adhesion and guidance or may not be appropriately oriented. Bundles of longitudinally-aligned electrospun fibers can also be inserted inside a cylindrical nerve guide to fill the lumen, but unlike channels, they do not confine nerve to particular paths (Clements et al. 2009; Lietz et al. 2006; Mauck et al. 2009; Yucel et al. 2010). Additionally, tight packing of these bundles may inhibit axon and Schwann cell migration. In contrast to existing electrospun nerve guides, our design creates a complex 3-dimensional construct with open channels to guide the nerve and Schwann cells between the fibrous substrate.

Fabrication

Our fabrication process successfully demonstrates proof of concept for a nerve guide constructed entirely of electrospun fibers. The two electrospun layers encapsulated the templates and exhibited sufficient interaction to prevent delamination. We believe that the insulating properties and smooth surface of the templates allow easy removal from the electrospun fibers without disrupting the channel architecture despite a large aspect ratio. Finally, the cylindrical shape was maintained by a circumferential sheath of fibers deposited around the outside.

Fibrous microstructure—A section of the 6-0 collagen nerve guide viewed by SEM (Fig 4A & B) demonstrates the structure of the electrospun fibers around the microchannels. This microfiber mesh creates an open network of paths for nutrient transport into and out of the channel. The fibers in Figure 4B show some artifact resulting from cutting. Thus, fiber morphology can be better evaluated from a flat sheet of the electrospun fibers (Fig4 E). This image shows smooth fibers of roughly uniform diameter. The unraveling of the coil as seen in Figure 4A was addressed in later guides by an electrospun sheath (Fig 4C) which fixes the guide in the circular shape. The circumferentially-oriented fibers of the sheath can be seen covering the layer of random fibers in Figure 4D.

Primary and secondary channels—Multi-channel guides fabricated with a range of diameters are shown in Figure 5. Figure 5A shows a nerve guide with 25 channels approximately 176 μm in diameter fabricated with 4-0 synthetic sutures. Although not homogenous in shape or dimension, an equivalent number of secondary channels double the channel density. Secondary channels adjacent to each primary channel were formed by the space between the primary channels and the flat mesh. The size of these secondary channels is affected by the ratio of the two electrospun layers and the template diameter. Secondary channels provide additional space for cell migration, but due to the inhomogeneity of these structures we focus on the primary channel. Figure 5B and C shows guides produced from 6-0 collagen and synthetic sutures respectively. Primary channels in these guides are more circular and the secondary channels more regular. One 10-0 guide was made for the purpose of demonstrating versatility of this method (Fig 5D). Only 10 channels were made since 10-0 sutures are very short and it requires many sutures to obtain the same number as larger sutures. Since the layer thickness was not adjusted for this design, the channels contribute very little open area for nerve growth and no secondary channels are present. As seen in the figure, 10-0 sutures do not act well as mandrels for rolling, resulting in loose rolling and the

large central lumen observed in this figure. Due to the manual steps involved with this process we recognize that there may be a minimum diameter that is feasible with the current technique. Although, we do not think that this will hinder the success of our design, we hope to improve the precision with more automated techniques in the future.

Channel diameter—Suture templating resulted in channel diameters 13 to 28 μm larger than the sutures used to create the channels. We hypothesize that electrospun fibers are not attracted to the sutures and are not deposited tightly around them, accounting for the diameter differential. Although initial work began with collagen sutures, synthetic sutures or fishing line were later used due to easier removal.

Layer thickness—The thickness of each electrospun layer can have drastic effects on the structure and mechanics of the guide. The mentality behind our design is to minimize the layer thickness to facilitate transport through the walls and maximize the number of microchannels available while still providing sufficient mechanical strength. Figure 3D &E shows how thinner walls guides are less defined and more susceptible to deformation during cutting compared to thicker guides in Figure 3F. Consequently, future work to increase open areas designated for cell adhesion will focus on increasing template spatial frequency, not decreasing wall thickness.

Porosity—Porosity was estimated using geometric calculations based on mass and volume of the final guide and the density of the PCL (1.145 g/cm^3). These volume calculations were supported by similar values obtained via a second set of calculations that used the V_1 and V_2, the 14% PCL polymer concentration, and the percent of the collector area used for making the guide. The total porosity and the percent contributed by the channels are reported in Figure 3. All guides in this sample set showed porosity above 85 percent. Additionally, void space between electrospun fibers contributed to the majority of porosity since the highest Pc was 16 percent. This supports the premise that our electrospun mats are highly porous and should be conducive to nutrient transport.

Reproducibility—As with any fabrication process, reproducibility is important. The current method contains two areas where variability can be introduced: electrospinning steps and manual steps. Achieving stable and consistent electrospinning conditions is essential to producing repeatable guides. Fiber diameter and morphology are known to be affected by electrospinning parameters which include acceleration voltages, polymer molecular weight, solution concentration, and humidity. One electrospinning complication that may arise is the formation of globs or nets of fibers depositing on the collector(Leach et al. 2011). These do not form tightly around the template and cause defects in the design. A second variation that can greatly influence the outcome of templated guides is uneven distribution fibers on the collector. If uneven deposition occurs, some regions will be thick while others are thin and weak. To facilitate more uniform distribution, the collector may be slowly moved during electrospinning.

Rolling the flat sheet to form the cylindrical guide is the primary step in which manual variation can affect the outcome. As is evident in Figure 5A & D, a large central lumen is formed if the guide is not rolled tight enough. Contrarily, if the guide is too tight, compressive forces deform the channel shape when the template is removed. This is especially significant for guides with thin layers (Fig. 3D). Additionally, template alignment is important for maintaining uniform spacing between channels.

Reproducibility can be achieved by maintaining consistent conditions between samples. These include electrospinning parameters (acceleration voltage, solvent and concentration of the polymer solution, distance, flow rate, humidity), thickness of fibrous mat, template size

and spacing, and rolling tightness. Three guides produced by the same electrospinning and template conditions were imaged and shown in Figure 3A-C to demonstrate reproducibility of this method. The channel shape and overall quality of the guides becomes more vulnerable to cutting damage as the layer thickness decrease. This is evident in the bottom panel (Fig 3D-F) where channels become more defined as the layer thicknesses increase.

Fabrication time—The time required to fabricate guides using this technique include both electrospinning and templating times. Electrospinning time depends on the rate of spinning and the volume spun. This step can range from approximately 5-30 minutes accordingly. The templating step depends on the number of templates used. Template stringing time is approximately five per minute. This can vary depending on the size of the template and the skill of the person.

Versatile fabrication process

Synthetic nerve guides offer two advantages over autografts and allografts: availability and customizability. Our method of electrospinning with micro-templating demonstrates customizability in many aspects of the design. Electrospinning is a versatile technique that allows tailoring of the fiber diameter and alignment by changing solution and process parameters (Ghasemi-Mobarakeh et al. 2008). Collagen and synthetic sutures of various sizes (6-0, 7-0, and 10-0) were used to demonstrate the ability to form channels with diameters ranging from 33-176μm (Fig 4). The available templates could theoretically be expanded to produce channels over the range of available template diameters: 10 μm with 11-0 to 800 μm with 6-0. However, as mentioned previously, we do not expect to be working in this range.

The number and spacing of sutures can also be altered to match the fascicle geometry of the nerve being replaced. Diameter and length of the guide can be increased by electrospinning wider meshes on larger collectors. Finally, this method is applicable with any electrospun polymer, where the stratified fabrication method permits different polymer to be used for each layer. Since electrospinning solutions can incorporate functional proteins or cells, we may be able to match mechanical properties or incorporate biochemical cues (Biazar et al. 2010; Jiang et al. 2006; Townsend-Nicholson and Jayasinghe 2006).

Fiber diameter—Parameters for fiber and channel diameter have yet to be optimized for our nerve guide. The size of the fibers with respect to that of the cell can affect how the cell senses and interacts with the substrate (Agarwal et al. 2008). The current electrospinning parameters produce a random mesh approximated by ImageJ measurements to be 2μm diameter fibers (Fig 4E). Control of diameter was not the focus of this work, but significant existing literature can be referenced to tightly control and measure diameter distribution over wide range. Endoneurium, perineurium, and epineurium of native nerve all contain bundles of longitudinally-aligned collagen fibrils ranging from 25-100nm in diameter (Gamble 1964). However, prior work studying nerve and Schwann cell migration on longitudinally-aligned fibers demonstrates that some directional control may be lost with the use of very small fibers (293nm) and that larger fibers (759 and 1325 nm) yield quickest migration. Thus, while fiber diameter for the current design may affect the cell attachment and infiltration, future work involving incorporation of aligned fibers within channels will rely heavily on a diameter that is optimal for topographical guidance.

Channel diameter—From existing literature, it is unclear whether channel diameters near that of fascicles (200-400μm) or individual axons (2.5-22μm) are more conducive to axon regeneration (Gustafson et al. 2009; Terzis and Smith 1990). Prior work has not demonstrated statistically significant differences for axonal growth depending on channel

size (Scott et al.). Although previous work with multi-channel guides showed that channels of small (12μm & 19μm) and (105 μm) medium diameter both supported rapid axon growth, small channels also restricted Schwann cell infiltration (Scott et al.). Consequently, our current method using medium-sized channels around 100μm may be appropriate.

Electrospun fibers permit schwann cells to populate the guide

These guides were designed for application in peripheral nerve repair, so initial in vitro work was performed with Schwann cells. Schwann cells are critical to creating a permissive environment preceding nerve repair via phagocytosis of debris, deposition of basal lamina, and release of neurotrophic factors(Gu et al. 2010). Although it is controversial whether Schwann cells precede axonal regeneration (Chen et al. 2005) (Yannas 2001)or follow axons into a lesion site (Brushart 2011; Kettenmann and Ransom 2005), Schwann cells are intricately involved in the regenerative process. For these reasons, tissue engineering approaches to nerve repair have incorporated Schwann cells from a variety of sources including autologous, allogeneic, cell lines, or stem cells (Gu et al. 2010). Consequently it is important that Schwann cells respond appropriately to the environment created by our nerve guide.

We demonstrated the feasibility of our design using PCL since it can easily be electrospun. Since PCL is a component of FDA-approved nerve guides, Neurolac, and has been established as a suitable biomaterial from prior peripheral nerve research (Kehoe et al. 2011) in vitro biocompatibility tests were not repeated in this research. We aimed simply to demonstrate that Schwann cells infiltrate into the interior of the guide along the microchannels. While PCL exhibits slow degradation which may be suitable for the slow regeneration of nerves (Bolgen et al. 2005), we acknowledge that high hydrophobicity and lack of functional groups may preclude PCL from use in our final design.

Guides for all in vitro culture were coated with laminin prior to cell seeding. PCL alone does not contain any functional groups or bioactive domains for cellular recognition. However, in the body most foreign surfaces are quickly coated by natural protein adsorption. To mimic the adhesion sites present in vivo, nerve guides were coated in laminin, a protein known to improve Schwann cell adhesion, proliferation, and survival(Chernousov et al. 2008).

SEM—Schwannoma cell adhesion and morphology on the fibrous electrospun substrate were observed after 8 days in culture. Images from SEM (Fig 4F) show the morphology of these cells on random electrospun fibers of the nerve guide interior. Cells on the random fibers appear to have rounded cell bodies sprawled out on top of the fibers. Cells adhere to random fibers via extension of several processes per cell but do not show any directional preference.

MTT—MTT results from seeded guides show absorbance readings close to that of one million cells. Actual MTT activity may be higher since the guide still contained areas of deep purple color that could not be freed despite mechanical disruption. This suggests that cells are not only alive but metabolically active. However, analysis of these results should consider that histology shows a high density of cells on the outside of the guide (Fig 7 C & D) and that MTT cannot provide insight on location of metabolically active cells. Furthermore, thick layers of Schwann cells becoming overconfluent in aggregates may begin to change phenotype and also skew results.

Live/Dead/DAPI—Live/Dead solutions were added to guides at 4 and 11 days (Data not shown). A layer of live cells were identified around the outside of the guide and only a few dead cells were seen evenly distributed throughout the entirety of the guide. DAPI staining

showed many more cells distributed throughout the central region of the guide. We believe that the majority of the cells are alive but lack staining by the calcein AM since it is hydrophobic and likely adsorbed by the large surface area of PCL fibers. The staining of dead cells throughout the guide suggests that the more hydrophilic nature of the ethidium homodimer permits it to diffuse more freely. Consequently, the Live/Dead staining was not useful for characterizing cell growth in our guides. Thus MTT was used for quantification while DAPI staining was used to qualitatively inspect distribution and number.

DAPI staining from longitudinal images reveal that Schwannoma cells can populate the entire length of the nerve guide (Fig 7C). By inspection, an increase in cell density can be observed from day 4 to day 11. This suggests cell proliferation within the guide channels, including the mid-section which has the least access to fresh media. Schwannoma cell migration and proliferation throughout the entire guide is further supported by increased cell density throughout channels in the transverse-sections of the nerve guides at the ends (Fig 7 B & D). These reveal that Schwannoma cells primarily reside within the channel lumens and gaps between layers with less penetration into the fibrous walls. This distribution pattern of cells within channels is also seen in longitudinal sections in Figure 7C. The localization of cells within the channel is consistent with literature reporting the scarcity of cell penetration into the interior of electrospun meshes (Nisbet et al. 2009).

We believe that the high surface area and porosity offered by electrospun structures enhances the cell penetration along the channels of the nerve guide. Additionally, open space offered by the channels provides regions of low growth resistance that serve to direct axons toward a single distal target. As supported by the in vitro cell culture, the diffusion permited by this fibrous mesh permits cell proliferation within even the central-most interior of the nerve guides (Fig 7). Additionally, the small size of voids between electrospun fibers restricts most cells from migrating into channel walls and minimizes influx of inflammatory cells from the surrounding tissue upon implantation. Electrospun fibers strike the balance between high interconnectivity that allows good mass transfer and small pathlength that confines Schwann cells and nerves within the channels.

Future work

This work is the first step in demonstrating a new design of synthetic nerve guides. Like any new technology, there are aspects awaiting further investigation. Two modifications that we believe are crucial involve transitioning to a more suitable biomaterial and automating the fabrication. Alternatives to PCL will be pursued in the future to increase hydrophilicity, introduce cell adhesion sites, and broaden degradation profile to match clinical needs. Ten-cycle compressive tests (not shown) demonstrate hysteresis after an initial plastic deformation. Thus to prevent channel collapse in future designs we will use an elastomer such as poly(glycerol sebacate) that increases elastic recovery (Sundback et al. 2005).

Variability introduced during the manual steps is a limitation that may be addressed using robotics in the future. Current methods involve templates that are extremely small and difficult to handle. Automating the process in the future should not only improve reproducibility, but also increase the channel density that can be achieved.

Conclusion

This paper reports a new electrospun construct containing a high density of aligned microchannels mimicking the fascicles in nerve. We demonstrate a high number of channels of defined size and shape within a porous structure. We believe these features distinguish our design from existing ones. We also demonstrate the repeatability and versatility of this method and begin to characterize cellular response. We will continue to focus on translating

this technology into clinically-useful products by testing the guides in a rat sciatic nerve model. Results from a pilot implantation demonstrate that the guide can anastamosed with 10-0 suture and maintains its shape without unrolling. In the future, we will couple this design with stimulatory cues such as aligned fibers within the aligned channels and growth factors.

Acknowledgments

This research is supported in part by an NIH grant # R21 EB008565. Rat Schwannoma cell line (ATCC CRL-2768) were kindly provided by Drs. Peter Crapo and Stephen Badylak. We thank Dr. Samer Zaky for performing the ethylene oxide sterilization.

References

Agarwal S, Wendorff JH, Greiner A. Use of electrospinning technique for biomedical applications. Polymer. 2008; 49(26):5603–5621.

Ao Q, Wang A, Cao W, Zhang L, Kong L, He Q, Gong Y, Zhang X. Manufacture of multimicrotubule chitosan nerve conduits with novel molds and characterization in vitro. J Biomed Mater Res A. 2006; 77(1):11–8. [PubMed: 16345091]

Biazar E, Khorasani MT, Montazeri N, Pourshamsian K, Daliri M, Rezaei M, Jabarvand M, Khoshzaban A, Heidari S, Jafarpour M. Types of neural guides and using nanotechnology for peripheral nerve reconstruction. Int J Nanomedicine. 2010; 5:839–52. [PubMed: 21042546]

Bolgen N, Menceloglu YZ, Acatay K, Vargel I, Piskin E. In vitro and in vivo degradation of non-woven materials made of poly(epsilon-caprolactone) nanofibers prepared by electrospinning under different conditions. J Biomater Sci Polym Ed. 2005; 16(12):1537–55. [PubMed: 16366336]

Bozkurt A, Brook GA, Moellers S, Lassner F, Sellhaus B, Weis J, Woeltje M, Tank J, Beckmann C, Fuchs P. In vitro assessment of axonal growth using dorsal root ganglia explants in a novel three-dimensional collagen matrix. Tissue Eng. 2007; 13(12):2971–9. [PubMed: 17937537]

Brushart TM. Nerve Repair. 2011

Campbell WW. Evaluation and management of peripheral nerve injury. Clin Neurophysiol. 2008; 119(9):1951–65. [PubMed: 18482862]

Cao H, McHugh K, Chew SY, Anderson JM. The topographical effect of electrospun nanofibrous scaffolds on the in vivo and in vitro foreign body reaction. J Biomed Mater Res A. 2009; 93(3): 1151–9. [PubMed: 19768795]

Chen YY, McDonald D, Cheng C, Magnowski B, Durand J, Zochodne DW. Axon and Schwann cell partnership during nerve regrowth. J Neuropathol Exp Neurol. 2005; 64(7):613–22. [PubMed: 16042313]

Chernousov MA, Yu WM, Chen ZL, Carey DJ, Strickland S. Regulation of Schwann cell function by the extracellular matrix. Glia. 2008; 56(14):1498–507. [PubMed: 18803319]

Chew SY, Mi R, Hoke A, Leong KW. Aligned Protein-Polymer Composite Fibers Enhance Nerve Regeneration: A Potential Tissue-Engineering Platform. Adv Funct Mater. 2007; 17(8):1288–1296. [PubMed: 18618021]

Chiona, V.; Tonda-Turo, C.; Ciardelli, G. Artificial Scaffold for Peripheral Nerve Reconstruction. In: Geuna, S.; Tos, P.; Battiston, B., editors. Essays on Peripheral Nerve Repair. 2009. p. 173-198.

Clements IP, Kim YT, English AW, Lu X, Chung A, Bellamkonda RV. Thin-film enhanced nerve guidance channels for peripheral nerve repair. Biomaterials. 2009; 30(23-24):3834–46. [PubMed: 19446873]

de Ruiter GC, Spinner RJ, Malessy MJ, Moore MJ, Sorenson EJ, Currier BL, Yaszemski MJ, Windebank AJ. Accuracy of motor axon regeneration across autograft, single-lumen, and multichannel poly(lactic-co-glycolic acid) nerve tubes. Neurosurgery. 2008; 63(1):144–53. discussion 153-5. [PubMed: 18728579]

Flynn L, Dalton PD, Shoichet MS. Fiber templating of poly(2-hydroxyethyl methacrylate) for neural tissue engineering. Biomaterials. 2003; 24(23):4265–72. [PubMed: 12853258]

Gamble HJ. Comparative Electron-Microscopic Observations on the Connective Tissues of a Peripheral Nerve and a Spinal Nerve Root in the Rat. J Anat. 1964; 98:17–26. [PubMed: 14109809]

George PM, Saigal R, Lawlor MW, Moore MJ, LaVan DA, Marini RP, Selig M, Makhni M, Burdick JA, Langer R, et al. Three-dimensional conductive constructs for nerve regeneration. J Biomed Mater Res A. 2009; 91(2):519–27. [PubMed: 18985787]

Ghasemi-Mobarakeh L, Prabhakaran MP, Morshed M, Nasr-Esfahani MH, Ramakrishna S. Electrospun poly(epsilon-caprolactone)/gelatin nanofibrous scaffolds for nerve tissue engineering. Biomaterials. 2008; 29(34):4532–9. [PubMed: 18757094]

Gu X, Ding F, Yang Y, Liu J. Construction of tissue engineered nerve grafts and their application in peripheral nerve regeneration. Prog Neurobiol. 2010

Gustafson KJ, Pinault GC, Neville JJ, Syed I, Davis JA Jr, Jean-Claude J, Triolo RJ. Fascicular anatomy of human femoral nerve: implications for neural prostheses using nerve cuff electrodes. J Rehabil Res Dev. 2009; 46(7):973–84. [PubMed: 20104420]

Hadlock T, Sundback C, Hunter D, Cheney M, Vacanti JP. A polymer foam conduit seeded with Schwann cells promotes guided peripheral nerve regeneration. Tissue Eng. 2000; 6(2):119–27. [PubMed: 10941207]

He L, Zhang Y, Zeng C, Ngiam M, Liao S, Quan D, Zeng Y, Lu J, Ramakrishna S. Manufacture of PLGA multiple-channel conduits with precise hierarchical pore architectures and in vitro/vivo evaluation for spinal cord injury. Tissue Eng Part C Methods. 2009; 15(2):243–55. [PubMed: 19196120]

Hu X, Huang J, Ye Z, Xia L, Li M, Lv B, Shen X, Luo Z. A novel scaffold with longitudinally oriented microchannels promotes peripheral nerve regeneration. Tissue Eng Part A. 2009; 15(11): 3297–308. [PubMed: 19382873]

Jha BS, Colello RJ, Bowman JR, Sell SA, Lee KD, Bigbee JW, Bowlin GL, Chow WN, Mathern BE, Simpson DG. Two pole air gap electrospinning: Fabrication of highly aligned, three-dimensional scaffolds for nerve reconstruction. Acta Biomater. 2011; 7(1):203–15. [PubMed: 20727992]

Jiang H, Hu Y, Zhao P, Li Y, Zhu K. Modulation of protein release from biodegradable core-shell structured fibers prepared by coaxial electrospinning. J Biomed Mater Res B Appl Biomater. 2006; 79(1):50–7. [PubMed: 16544305]

Kehoe S, Zhang XF, Boyd D. FDA approved guidance conduits and wraps for peripheral nerve injury: A review of materials and efficacy. Injury. 2011

Kettenmann H, Ransom BR. Neuroglia. 2005

Kim YT, Haftel VK, Kumar S, Bellamkonda RV. The role of aligned polymer fiber-based constructs in the bridging of long peripheral nerve gaps. Biomaterials. 2008; 29(21):3117–27. [PubMed: 18448163]

Leach MK, Feng ZQ, Tuck SJ, Corey JM. Electrospinning fundamentals: optimizing solution and apparatus parameters. J Vis Exp. 2011; (47)

Lietz M, Dreesmann L, Hoss M, Oberhoffner S, Schlosshauer B. Neuro tissue engineering of glial nerve guides and the impact of different cell types. Biomaterials. 2006; 27(8):1425–36. [PubMed: 16169587]

Madaghiele M, Sannino A, Yannas IV, Spector M. Collagen-based matrices with axially oriented pores. J Biomed Mater Res A. 2008; 85(3):757–67. [PubMed: 17896767]

Madduri S, Papaloizos M, Gander B. Trophically and topographically functionalized silk fibroin nerve conduits for guided peripheral nerve regeneration. Biomaterials. 2010; 31(8):2323–34. [PubMed: 20004018]

Mauck RL, Baker BM, Nerurkar NL, Burdick JA, Li WJ, Tuan RS, Elliott DM. Engineering on the straight and narrow: the mechanics of nanofibrous assemblies for fiber-reinforced tissue regeneration. Tissue Eng Part B Rev. 2009; 15(2):171–93. [PubMed: 19207040]

Nisbet DR, Forsythe JS, Shen W, Finkelstein DI, Horne MK. Review paper: a review of the cellular response on electrospun nanofibers for tissue engineering. J Biomater Appl. 2009; 24(1):7–29. [PubMed: 19074469]

Noble J, Munro CA, Prasad VS, Midha R. Analysis of upper and lower extremity peripheral nerve injuries in a population of patients with multiple injuries. J Trauma. 1998; 45(1):116–22. [PubMed: 9680023]

Schlosshauer B, Dreesmann L, Schaller HE, Sinis N. Synthetic nerve guide implants in humans: a comprehensive survey. Neurosurgery. 2006; 59(4):740–7. discussion 747-8. [PubMed: 17038939]

Schmidt CE, Leach JB. Neural tissue engineering: strategies for repair and regeneration. Annu Rev Biomed Eng. 2003; 5:293–347. [PubMed: 14527315]

Scott JB, Afshari M, Kotek R, Saul JM. The promotion of axon extension in vitro using polymer-templated fibrin scaffolds. Biomaterials. 32(21):4830–9. [PubMed: 21492932]

Stokols S, Sakamoto J, Breckon C, Holt T, Weiss J, Tuszynski MH. Templated agarose scaffolds support linear axonal regeneration. Tissue Eng. 2006; 12(10):2777–87. [PubMed: 17518647]

Stokols S, Tuszynski MH. The fabrication and characterization of linearly oriented nerve guidance scaffolds for spinal cord injury. Biomaterials. 2004; 25(27):5839–46. [PubMed: 15172496]

Sundback C, Hadlock T, Cheney M, Vacanti J. Manufacture of porous polymer nerve conduits by a novel low-pressure injection molding process. Biomaterials. 2003; 24(5):819–30. [PubMed: 12485800]

Sundback CA, Shyu JY, Wang Y, Faquin WC, Langer RS, Vacanti JP, Hadlock TA. Biocompatibility analysis of poly(glycerol sebacate) as a nerve guide material. Biomaterials. 2005; 26(27):5454–64. [PubMed: 15860202]

Terzis; Smith, DH. The peripheral nerve. In: Smith, K., editor. Structure, function, reconstruction. New York: Raven Press; 1990.

Townsend-Nicholson A, Jayasinghe SN. Cell electrospinning: a unique biotechnique for encapsulating living organisms for generating active biological microthreads/scaffolds. Biomacromolecules. 2006; 7(12):3364–9. [PubMed: 17154464]

Wang A, Ao Q, Cao W, Yu M, He Q, Kong L, Zhang L, Gong Y, Zhang X. Porous chitosan tubular scaffolds with knitted outer wall and controllable inner structure for nerve tissue engineering. J Biomed Mater Res A. 2006; 79(1):36–46. [PubMed: 16758450]

Wang CY, Zhang KH, Fan CY, Mo XM, Ruan HJ, Li FF. Aligned natural-synthetic polyblend nanofibers for peripheral nerve regeneration. Acta Biomater. 2010

Wang DY, Huang YY. Fabricate coaxial stacked nerve conduits through soft lithography and molding processes. J Biomed Mater Res A. 2008; 85(2):434–8. [PubMed: 17701972]

Yan, H.; Zhang, F.; Chen, M.; Lineaweaver, W. Conduit Luminal Additives for Peripheral Nerve Repair. In: Geuna, S.; Tos, P.; Battiston, B., editors. Essays on Peripheral Nerve Repair. 2009. p. 173-198.

Yang F, Murugan R, Wang S, Ramakrishna S. Electrospinning of nano/micro scale poly(L-lactic acid) aligned fibers and their potential in neural tissue engineering. Biomaterials. 2005a; 26(15):2603–10. [PubMed: 15585263]

Yang Y, De Laporte L, Rives CB, Jang JH, Lin WC, Shull KR, Shea LD. Neurotrophin releasing single and multiple lumen nerve conduits. J Control Release. 2005b; 104(3):433–46. [PubMed: 15911044]

Yannas IV. Tissue and organ regeneration in adults. 2001

Yao L, de Ruiter GC, Wang H, Knight AM, Spinner RJ, Yaszemski MJ, Windebank AJ, Pandit A. Controlling dispersion of axonal regeneration using a multichannel collagen nerve conduit. Biomaterials. 2010; 31(22):5789–97. [PubMed: 20430432]

Yao L, O'Brien N, Windebank A, Pandit A. Orienting neurite growth in electrospun fibrous neural conduits. J Biomed Mater Res B Appl Biomater. 2009; 90(2):483–91. [PubMed: 19130615]

Yucel D, Kose GT, Hasirci V. Tissue Engineered, Guided Nerve Tube Consisting of Aligned Neural Stem Cells and Astrocytes. Biomacromolecules. 2010

Zhang Y, Luo H, Zhang Z, Lu Y, Huang X, Yang L, Xu J, Yang W, Fan X, Du B. A nerve graft constructed with xenogeneic acellular nerve matrix and autologous adipose-derived mesenchymal stem cells. Biomaterials. 2010; 31(20):5312–24. [PubMed: 20381139]

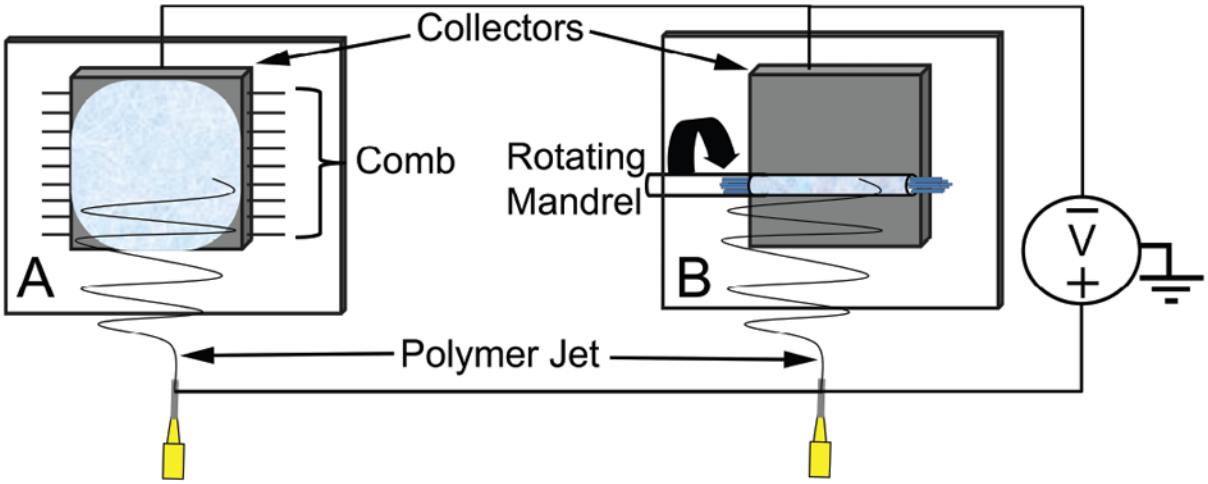

Figure 1.
Diagram of (A) stationary and (B) rotating electrospinning. (A) A stationary electrospinning set-up is used to produce a random fiber mesh. A polymer solution is pumped from syringe at a constant rate. A positive voltage is attached to syringe needle; a negative voltage is attached to an aluminum collector plate. The positively-charged polymer dries to form a thin fiber during flight toward the negatively-charged collection plate. (B) Rotational electrospinning set-up is used to produce radially-aligned fibers. Same process as stationary electrospinning is used except the fibers are deposited on a mandrel rotating in front of the collector.

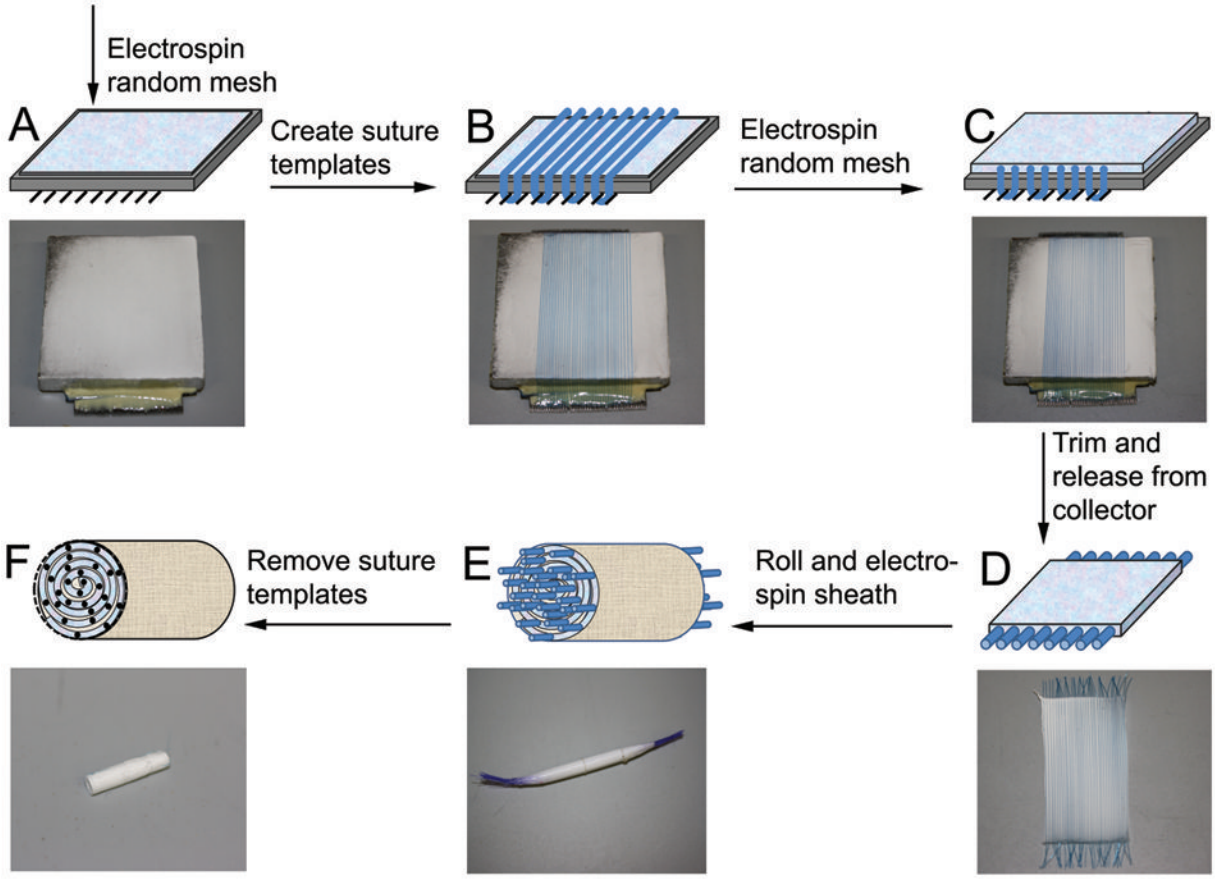

Figure 2.

Fabrication scheme for suture-templated electrospinning nerve guide (A) Deposit a thin layer (V_1) of random electrospun PCL fibers via stationary electrospinning setup. (B) Create channel template by stringing aligned sutures across first PCL layer and attaching to combs on sides of the collector. (C) Deposit second thin layer (V_2) of random electrospun PCL fibers via stationary setup. (D) After drying excess solvent in vacuum, cut sutures on both ends and trim flat sheet to length. (E) Roll up nerve guide and secure. Electrospin aligned PCL sheath around outside of guide by rotating electrospinning set-up. The template strands of one end of the nerve guide are placed in a tube and secured by parafilm. This is rotated at 60rpm in front of collector plate as 50 μl of aligned fibers are deposited around the exposed region. (F) Sutures are manually removed. Electrospun nerve guide is soaked in water to allow penetration and guide is cut after freezing on dry ice.

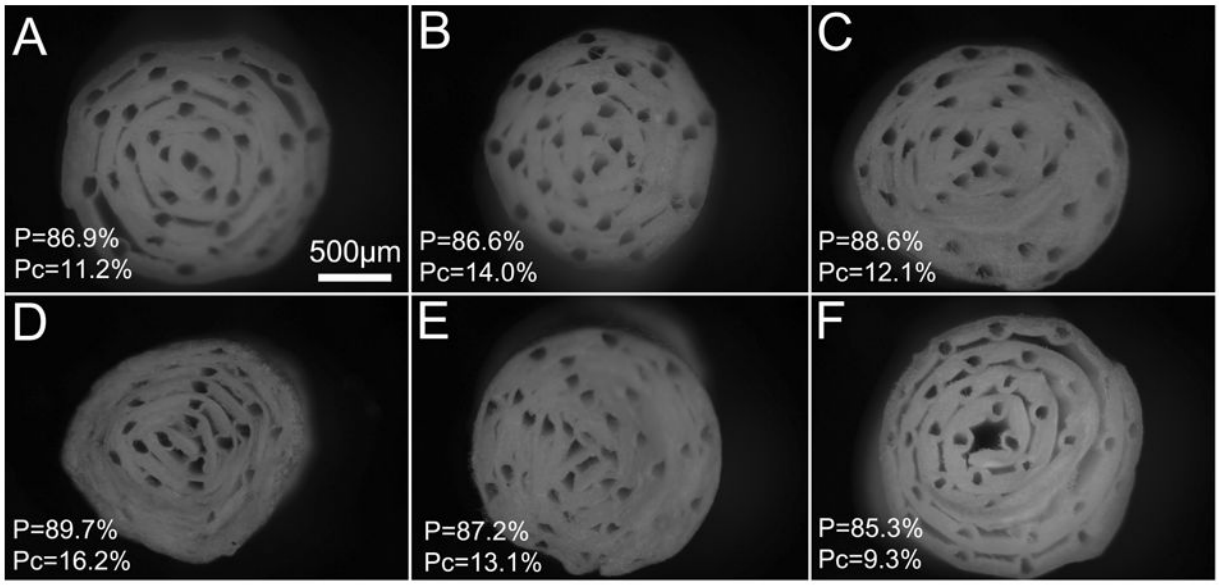

Figure 3.

Optical images of transverse-sections of multi-channel guides of different layer thickness and 35 templates (100 μm diameter). Total porosity (P) and percent channel porosity (Pc) is reported for each guide. (A-C) V_1/V_2=75 μL, (D) V_1/V_2=40, (E) V_1=40/V_2=100, (F) V_1/V_2=100.

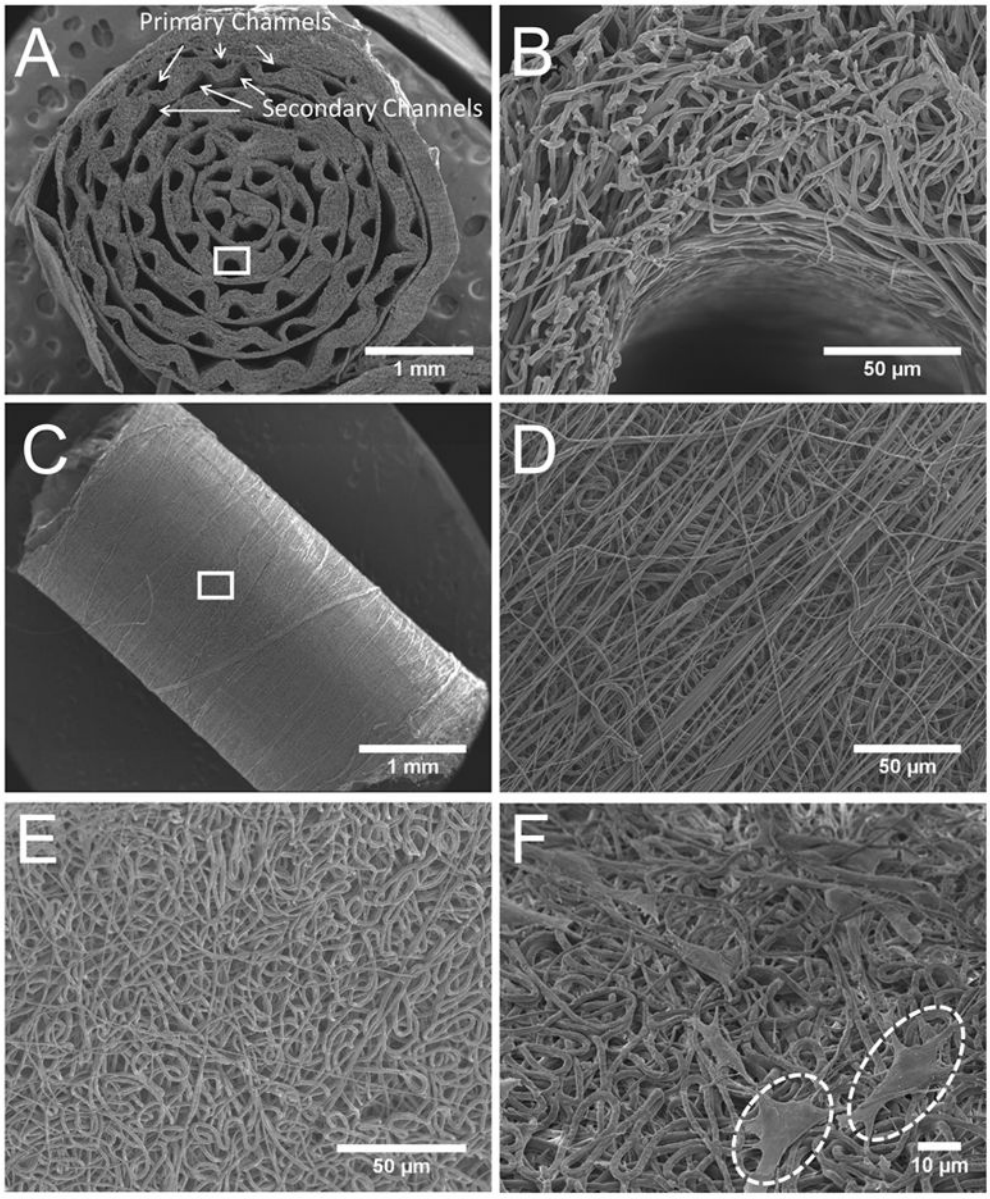

Figure 4.
SEM images of microchannels and microfibers in the nerve guides. (A and B) Transverse-section of nerve guide with aligned channels at 25 and 650 X magnification. (C and D) Outside of rolled nerve guide sealed with an electrospun sheath (Shown at 25 and 500 X magnification). (E) Top view of randomly-oriented fiber mat before rolling to form guide. (F) Schwannoma cells on random fiber electrospun fibers inside nerve guide after in vitro culture. Two cells are highlighted with circles.

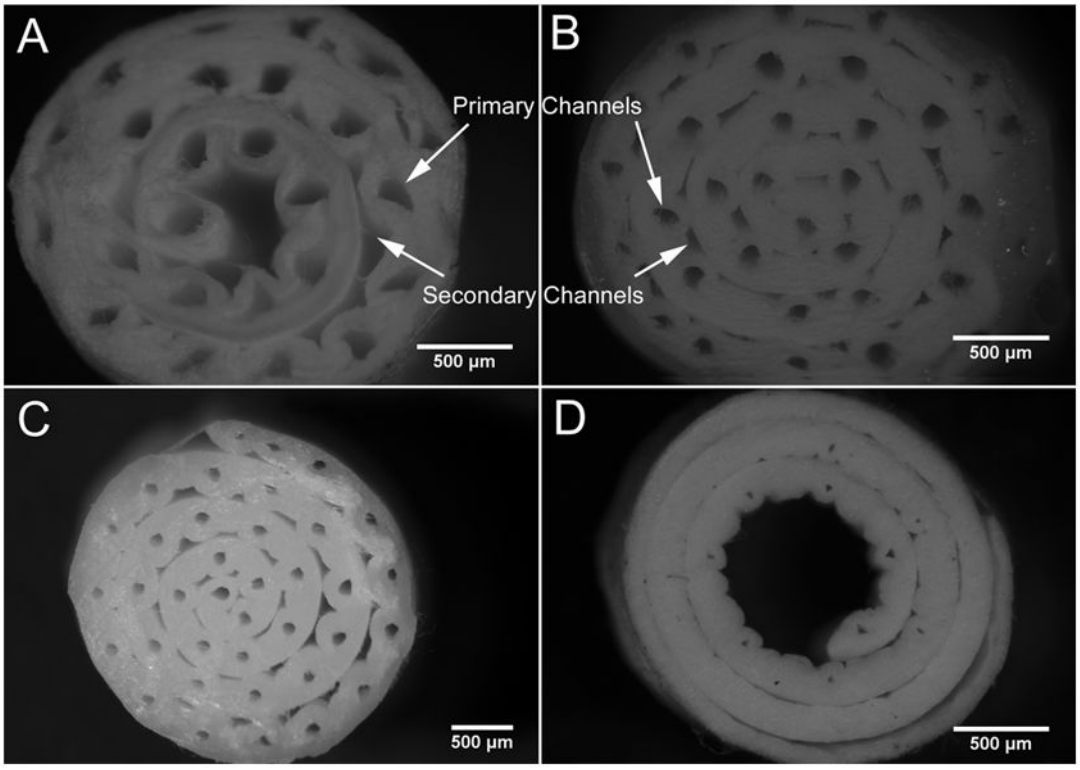

Figure 5.
Optical images of multi-channel guides with varying channel diameters. The various guides are not optimized, but rather are used to demonstrate the different diameters achievable using the templating method. Nerve guide fabricated with: (A) 4-0 synthetic sutures (150μm) to produce channels 176 ± 39 μm in diameter; (B) 6-0 collagen sutures (100μm) to produce channels 117 ± 11 μm in diameter; (C) 6-0 synthetic sutures (70μm) to produce channels 98 ± 9 μm in diameter; and (D) 10-0 synthetic sutures (20μm) to produce channels 33 ± 6 μm in diameter. Scale bar = 500 μm.

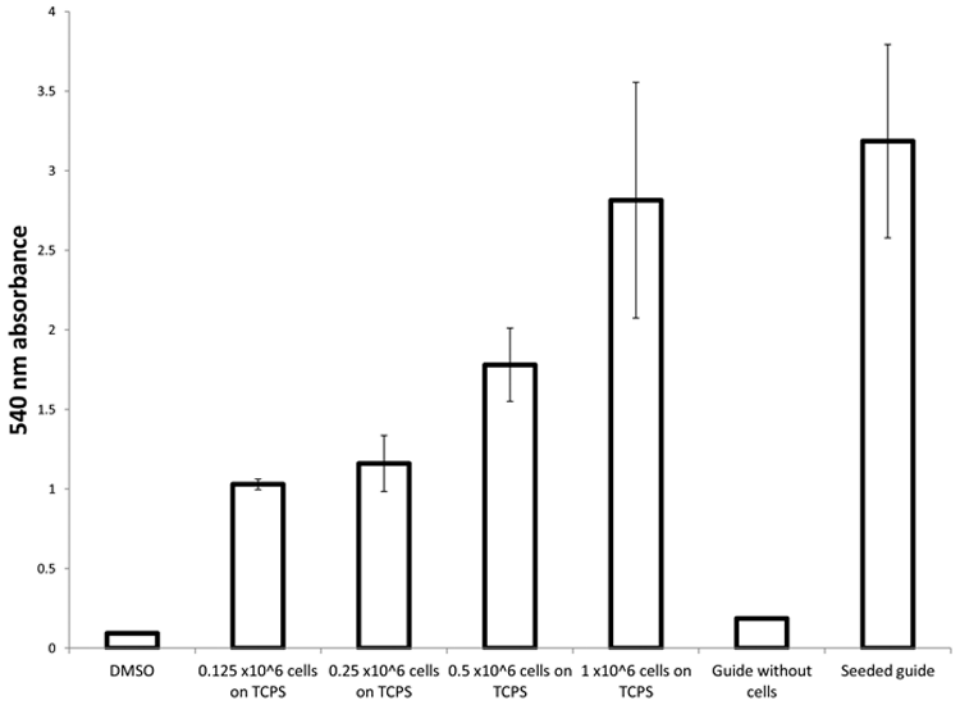

Figure 6.

Absorbance was read at 540nm to measure solublized MTT in DMSO following conversion by cellular metabolism. Absorbance readings were measured in triplicate for each sample (n=3).

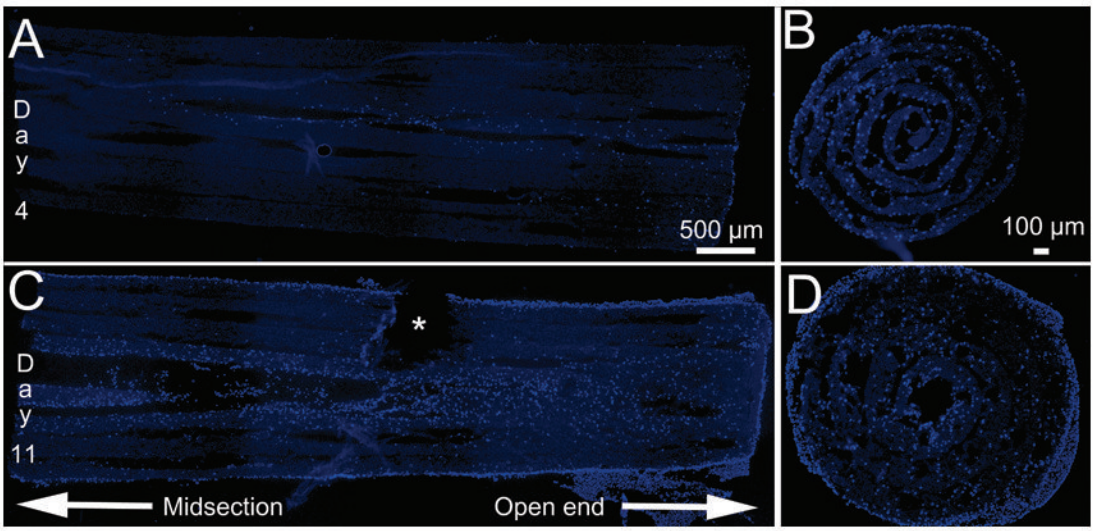

Figure 7.

DAPI staining reveals the longitudinal and transverse distribution of Schwannoma cell nuclei in the multi-channel nerve guide. (A) Longitudinal section after 4 days in culture. (B) Transverse section at open end after 4 days in culture. (C) Longitudinal section after 11 days in culture. Asterisk indicates tear caused by sectioning. (D) Transverse section at open end after 11 days in culture. Note: Fluorescent look up table (LUT) was adjusted to make nerve guide visible.